

FATIGUE CRACK PROPAGATION IN THE VICINITY OF WELD-DEPOSITS
IN HIGH-STRENGTH, STRUCTURAL STEEL

J.E.M. Braid and J.F. Knott

Department of Metallurgy and Materials Science,
University of Cambridge, Cambridge, U.K.

ABSTRACT

The propagation of fatigue-cracks has been studied in specimens of HY-80 steel containing "bead-in-groove" welds using constant applied loading and constant applied stress-intensity. Under constant applied stress-intensity conditions, increases in growth-rate were observed in parent-plate material and decreases were observed in the "fine-grain" and "coarse-grain" heat affected zone (HAZ) regions. It was found that there was little effect of microstructure on crack propagation-rates and the observed effects in the welded specimens were attributed to residual stresses. Preliminary measurements of residual stress have been made and a distribution is presented. The effect of this distribution on crack propagation-rates is analysed, using fracture mechanics.

KEYWORDS

Fatigue; Fatigue crack propagation rates; Welds; Residual stress; Simulated heat-affected-zone; Stress intensity; Sulphide inclusions; Redistribution of Residual Stresses.

INTRODUCTION

Current fatigue-design rules for welded joints are based on experimental S-N curves, whose positions vary with joint configuration (Maddox, 1971). This variation of fatigue performance with configuration could be attributed to differences in likely defect-content, in residual-stress distribution, or in both. The fatigue life of a welded joint (particularly class D or lower, (Maddox, 1971)) is almost entirely controlled by propagation from pre-existing defects, but the extent to which residual-stresses affect crack propagation rates, particularly at low applied-stress levels, is not entirely clear. Certainly, S-N curves for joints show pronounced scatter at low stress levels, and it would be of considerable practical value if such scatter could be explained on a physical basis, because the testing of complicated weldments at low stress levels is an expensive and time-consuming process. The aim of the work described in the present paper was therefore to examine possible effects of residual-stress on fatigue-crack propagation in a well-controlled system.

MODEL

To serve as a first experimental model, the weld was simplified to that of a "bead-in-groove" deposit in HY-80 steel, the composition and mechanical properties of which are given in Table 1. Notched, 4-point bend specimens were machined from the plate with the notch directly opposite the weld (diagram included in Fig. 3). Fatigue-crack propagation tests were performed under constant applied cyclic loading at $R = 0.2$ and constant applied cyclic stress intensity of $\Delta K = 20, 30$ and $40 \text{ MNm}^{-3/2}$. The crack lengths were measured using the D.C. potential-drop technique (Ritchie, Garrett and Knott, 1971).

As a crack grows from the notch it passes successively from parent-plate into fine- and coarse-grain heat-affected-zone (HAZ) microstructures and then into weld metal. The effects of the change in microstructure were examined by propagating cracks through specimens of parent-plate microstructure, or heat-treated to simulate the coarse-grain and fine-grain HAZ microstructures. The heat-treatment involved the application to bulk specimens of a thermal cycle similar to that produced by welding, adjusted to ensure matching of the microstructure and grain size to that of the weld HAZ. The testpieces were clamped between two sets of water-cooled copper blocks and an R.F. induction coil and concentrator were located around the notch area to provide the heat input. The resulting mean grain size was $210\mu\text{m}$ for the coarse-grain condition and $12\mu\text{m}$ for the fine-grain condition. The variation in grain-size across the specimen thickness was less than 10% for the coarse-grain condition and even less for the fine-grain condition. These grain-sizes compare well with the mean grain-sizes of $229\mu\text{m}$ and $16\mu\text{m}$ for coarse- and fine-grain HAZ microstructures in the "bead-in-groove" welds. The mean grain size of the parent-plate was $87\mu\text{m}$.

EXPERIMENTAL RESULTS

Fatigue-crack growth-rate curves under constant applied cyclic loading for parent-plate and HAZ-simulated specimens are shown in Fig. 1 together with selected constant ΔK results, corrected for the R ratio of 0.2. There is little difference between the crack growth-rates in coarse- and fine-grain simulated HAZ microstructures, although both are slightly faster than in the parent-plate microstructure. No effect of K_{mean} can be discerned for the parent-plate or simulated HAZ microstructure. The values of the Paris exponent, m , are 2.10, 2.22 and 2.56 for parent-plate, fine-grain and coarse-grain microstructures respectively. A "bead-in-groove" weld specimen gave a Paris exponent of 2.0. The values of threshold stress intensity, ΔK_{th} , were obtained for simulated coarse- and fine-grain HAZ microstructures at $R = 0.05, 0.2, 0.5$ and 0.7 and are shown in Fig. 2. There appears to be little effect of R ratio on ΔK_{th} for the coarse-grain condition but a definite effect can be seen for the fine-grain condition at values of R less than 0.5, these being higher than those for the coarse-grain condition.

The results of constant, applied, cyclic stress-intensity tests for the "bead-in-groove" weld specimens are given in Fig. 3, for $K_{\text{mean}} = 25 \text{ MNm}^{-3/2}$, as graphs of da/dN vs. a/W . In all cases, under conditions of constant applied stress intensity, when the crack grew from the parent-plate into the HAZ and into the weld, da/dN decreased when the crack first entered the HAZ. The results of constant applied stress-intensity propagation-tests on parent-plate and simulated coarse- and fine-grain HAZ microstructures are also given in Fig. 3.

The parent-plate growth-rates are slower than those in the parent-plate of the "bead-in-groove" weld testpieces. The growth-rates in fine-grain simulated HAZ microstructure are the same as, or slightly higher than, those for the corresponding fine-grain HAZ microstructure in the "bead-in-groove" weld specimens.

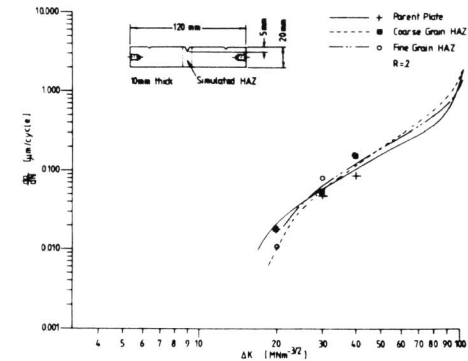


Fig. 1. da/dN vs ΔK

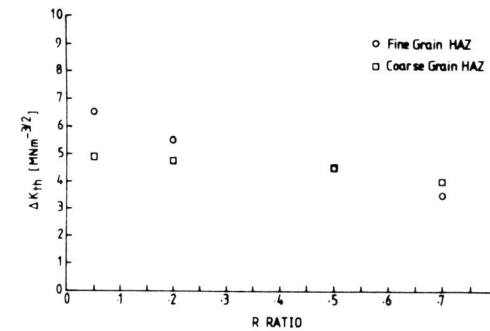


Fig. 2. ΔK_{th} vs R ratio

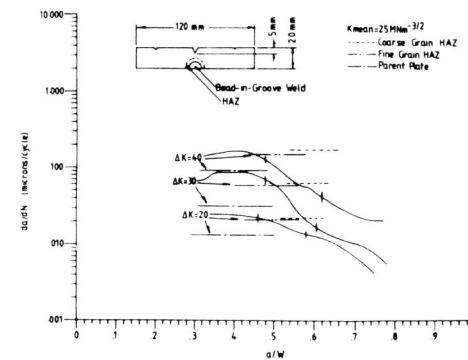


Fig. 3. da/dN vs a/W , constant applied stress intensity



Fig. 4. Fatigue surface showing plate MnS particle

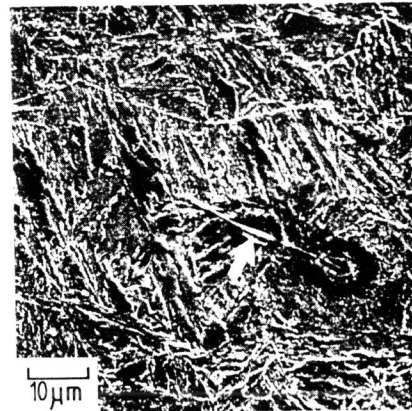


Fig. 5. HY-80 microstructure: arrow indicates MnS particle - etched 2% nital

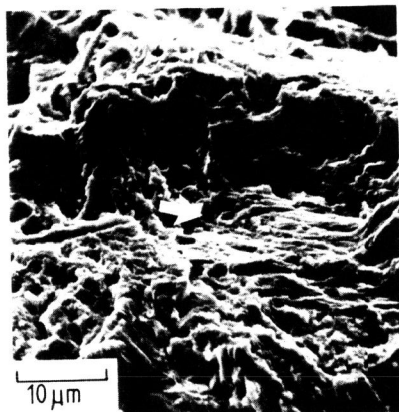


Fig. 6. Fatigue surface: coarse-grain HAZ - MnS particle indicated with arrow

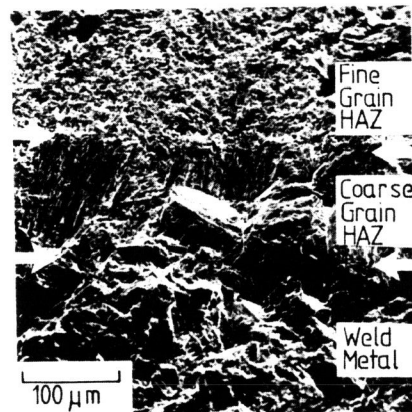


Fig. 7. Fatigue surface: "bead-in-groove" weld specimen

Values of da/dN for simulated coarse-grain microstructures are much higher than those in coarse-grain microstructure in the "bead-in-groove" weld specimens.

Scanning electron microscopy and an energy-dispersive-analysis of X-rays (EDS) revealed the presence of large plates of MnS inclusions as shown in Figs. 4 and 5. These are oriented perpendicular to the fatigue surface and are dispersed randomly across the grains in parent-plate and fine-grain HAZ microstructures (both actual and simulated). Fatigue-fracture rarely propagates across these plate sulphides but proceeds by shear along the weaker particle/matrix interface, as seen in Fig. 4. Few MnS particles were observed in the coarse-grain HAZ microstructure (either actual or simulated) and those observed were spherical particles approx. 0.75 μm diameter, resulting from re-solution at temperatures above 1300°C and re-precipitation in the matrix as shown in Fig. 6 (Segal, 1975). Mechanical dislodgement of these particles at a fatigue surface is also much easier than for the plate morphology and it is expected that this is the reason for the very low occurrence of these particles on the fatigue surface.

Figure 7 shows a typical fatigue surface in a "bead-in-groove" weld specimen. Fatigue-crack propagation in parent-plate, fine-grain HAZ (actual and simulated) and weld-metal was by a ductile fibrous mechanism which is compatible with the Paris exponent of $m = 2.5$ (Ritchie and Knott, 1973). The reversed plastic-zone-size varied between 52.6 μm and 210 μm, i.e. 1 to 2.5 times the parent-plate grain-size, or 4.5 to 17.5 times the fine-grain HAZ grain-size. Growth in the coarse-grain HAZ microstructure can be seen (Figs. 6 and 7) to be of a transgranular, ductile striation mechanism where the reversed plastic-zone-size is 0.25 to 1 times the grain size.

DISCUSSION

The behaviour shown by the test results can be analysed in terms of three possible parameters:

- Microstructure through which the crack is propagating
- Size, concentration and nature of inclusions present
- Presence of residual stresses.

The results shown in Fig. 1 indicate that there is little effect of microstructure on crack propagation-rates. One possible effect could be that due to grain size, in which a fatigue-crack is retarded at a grain-boundary and must reinitiate in the next grain. For a decreasing grain-size, the resistance of slip transference between grains increases and hence crack propagation would be expected to decrease, an effect opposite to that observed. At stress-intensities near threshold this would, however, cause an increase in ΔK_{th} , as observed in Fig. 2 for the fine-grain HAZ condition for R less than 0.5.

The results shown in Fig. 1 also indicate that there is little effect of inclusion content/morphology on crack propagation-rates. Growth past the MnS inclusion plates occurs by decohesion of the particle/matrix interface. This type of mechanism would generally act to blunt the crack tip, causing the crack propagation-rate to be lower than that in the absence of such inclusions. This effect is also opposite to that observed. At stress-intensities near threshold the effect could cause an increase in ΔK_{th} , as observed in the fine-grain condition in Fig. 2 for R less than 0.5.

From the discussion above it is evident that microstructure and inclusion-content have little effect on crack growth-rates except at stress-intensities near threshold. The decrease in propagation rates observed in tests under constant applied stress-intensity is therefore attributed to welding residual-stresses.

The residual-stresses arise from two basic sources; shrinkage and solid-state phase-transformations. Resulting general distributions for various geometries have been discussed at length by various authors (Macherauch and Wohlfahrt, 1978; Grey, Spence and North, 1975). Of the two sources, shrinkage tends to dominate and a first approximation, based on shrinkage, for a residual stress distribution for the "bead-in-groove" situation is given in Fig. 8(a) (Grey, Spence and North, 1975). Preliminary measurements of the through-thickness residual-stress distribution have been made using a modification of the slicing technique of Rosenthal and Norton (1945). The results are shown in Fig. 8(b). As can be seen, the stress-distribution is of the same general pattern as that predicted in Fig. 8(a). The bar used in the preliminary measurements was from the same welded plate as the fatigue specimens but was of a different geometry (the a_0/W ratio was 0.48 compared with 0.25) and the measuring gauge was some 18mm away from the weld/crack centre-line. Because of this, it is expected that the distribution along the line of fatigue-crack propagation in the "bead-in-groove" tests should be of the same general shape as that observed, but of much greater intensity, since transverse welding residual stresses fall to zero rapidly with increasing distance from the weld. Measurement of the distribution along the notch/weld centre-line is currently in progress, using a specimen from the fatigue-test series.

As shown in Fig. 8(a) the source of the residual-stress is the tensile field caused by plastic deformation of the weld metal, which accommodates the shrinkage during cooling. The rest of the distribution is theoretically an elastic response, being tensile in the parent-plate in front of the notch and compressive in the HAZ. For the geometry of the test specimens the source of the distribution is remote from the crack-tip until the crack has penetrated the weld metal. It would therefore be expected that, as a crack propagates, the residual stress should re-distribute ahead of the crack tip, but little relaxation should occur until the crack nears the source of the residual stresses (Underwood, Pook and Sharples, 1977).

Underwood, Pook and Sharples (1977) studied fatigue-crack propagation in a known residual stress field where the source of the residual stresses (plastic deformation due to indentation) was remote from the crack. For long cracks the residual stress field was accounted for, in terms of an "effective" alternating stress intensity, ΔK_c :

$$\Delta K_c = \Delta K_{\text{appl}} + K_R \tag{1}$$

where ΔK_{appl} is the applied value and K_R is due to the residual stress. Using this type of analysis in the present case, values of ΔK_c were obtained by comparing bulk material tests (Fig. 1) and "bead-in-groove" tests (Fig. 3). For applied $\Delta K = 30 \text{ MNm}^{-3/2}$, Fig. 3, growth rates of 0.087, 0.06 and 0.019 $\mu\text{m}/\text{cycle}$ for parent-plate, fine-grain and coarse-grain HAZ microstructures respectively were used to obtain, from Fig. 1, K_c values of 35.5, 30.0 and 22 $\text{MNm}^{-3/2}$. Hence K_R is deduced to vary from 5.5 to -8.0 $\text{MNm}^{-3/2}$ in the direction of propagation.

Underwood, Pook and Sharples (1977) used a simple expression for obtaining K_R from the residual stress data as

$$K_R = \sigma_{\text{Rave}} \sqrt{\pi a} \tag{2}$$

which yields stresses of 38.8 MPa to -42.09 for the $\Delta K = 30$ results. Although these are of the same order and in the correct location as the stresses in Fig. 8(b), the use of such a simple expression is open to question. A more accurate integral form, which would account for the actual distribution would be

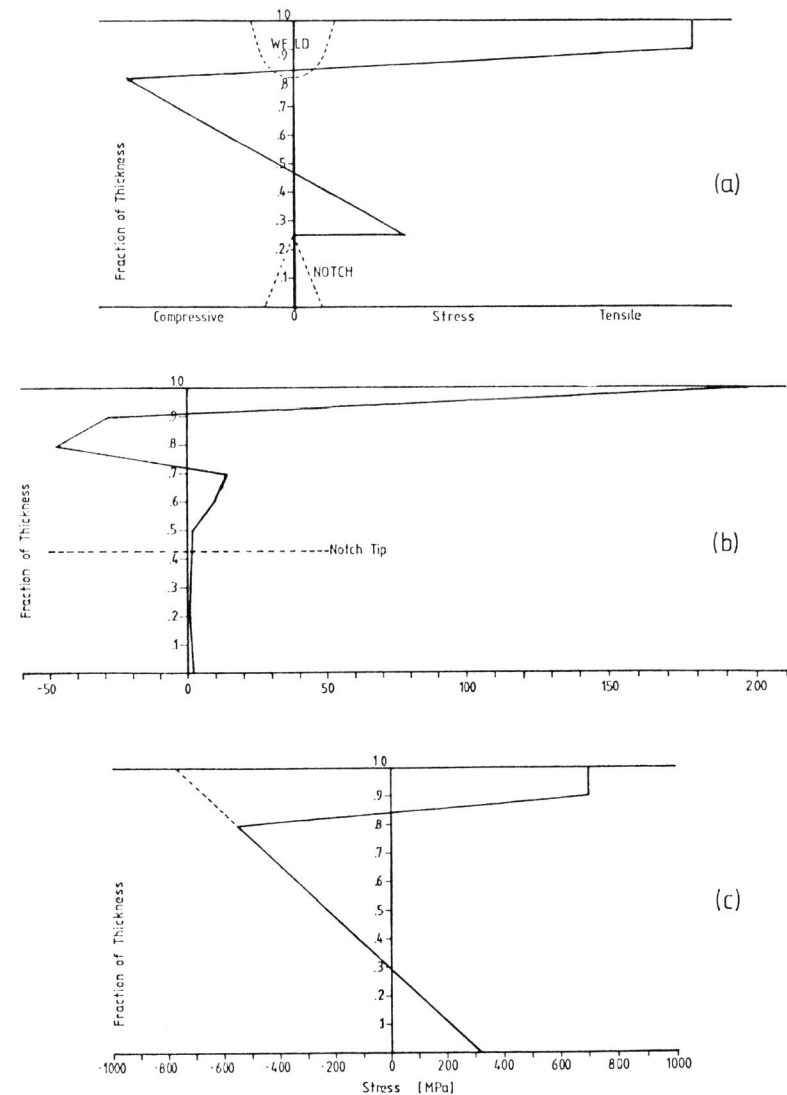


Fig. 8. Residual stress distribution: a) Theoretical from shrinkage considerations, b) Preliminary measured distribution and c) Distribution derived from data for $\Delta K = 30$ (Fig. 3).

$$K = \frac{2\sqrt{a}}{\pi} \int_0^a \frac{\sigma(t)}{\sqrt{a^2 - t^2}} dt \quad (3)$$

where $\sigma(t)$ is the value of the residual stress at a position t . Assuming that the residual stress distribution varies linearly through the thickness (for the elastic response only) and using the K_R values obtained above, a distribution, given in Fig. 8(c), can be derived using the above equation. Using this distribution growth rates for other loading cases can be predicted. For example, at a/W of 0.4, equation (3) gives $K_R = 4.13 \text{ MNm}^{-3/2}$ and at a $\Delta K_{\text{appl}} = 40 \text{ MNm}^{-3/2}$, $\Delta K_c = 44.13$. From Fig. 1, da/dN for $\Delta K_R = 40 \text{ MNm}^{-3/2}$ is $0.13 \mu\text{m}/\text{cycle}$. If ΔK is "corrected" to 44.13 the value becomes $0.154 \mu\text{m}/\text{cycle}$ which agrees much more closely with the value of $0.165 \mu\text{m}/\text{cycle}$ from Fig. 3, for $\Delta K_{\text{appl}} = 40 \text{ MNm}^{-3/2}$.

In general it might be expected that the residual stresses would redistribute ahead of the crack tip as the crack grows. If this occurred, however, the residual stresses at the crack tip would always be tensile, resulting in growth-rates constantly higher than those in bulk material. Since the propagation rates in "bead-in-groove" tests decrease below those in bulk material, it would indicate that redistribution was not occurring. Theoretical predictions from a superposition of applied and residual stresses using equation (3) were made by Adams (1973) and compared well with his experimental results in centre-cracked plates with two weld-passes (symmetrically disposed on each side of the crack). Redistribution was not considered in his analysis on the grounds that the crack remained in a compressive field which extended from the centre-notch to the weld (residual-stress source). Underwood, Pook and Sharples (1977) took redistribution of the elastic response stresses into account and had considerable success in describing their difference in growth-rates from bulk material data. Here again, the residual-stress field at the notch-tip was compressive and remained compressive during the propagation tests by redistribution. By consideration of the remote nature of the residual stress source and the geometry of the "bead-in-groove" weld specimens in the present tests, redistribution is expected but fatigue crack propagation rates indicate that this is not occurring. Further investigations are underway, including a more accurate measurement of the residual stress distribution, to attempt to solve this dilemma.

CONCLUSIONS

A study of fatigue-crack propagation has been conducted for constant applied cyclic-loading and constant applied cyclic stress-intensity in notched bend specimens of HY-80 steel containing a "bead-in-groove" weld deposit. The crack progressed from parent-plate, through fine- and coarse-grain HAZ and into the weld metal. Under conditions of constant applied ΔK , the crack grows faster in the parent-plate microstructure and then progressively slower, as it passes through the HAZ and into the weld metal. Propagation-rates and threshold stress-intensities were also obtained in specimens of bulk material of parent-plate and fine- and coarse-grain HAZ microstructures. The tests in the bulk material indicate that microstructure and inclusion content have little effect on crack propagation-rate except at stress intensities near threshold. The observed decrease in propagation rates was therefore attributed to the presence of residual stresses.

Preliminary measurements of through-thickness residual stresses have resulted in a distribution of a form similar to that expected due to the shrinkage of the weld upon cooling. It was expected that during crack growth the residual-stresses

would redistribute ahead of the crack tip since the source of the residual stresses was remote from the crack. This would, however, have resulted in a continuous growth of the crack at higher rates than in bulk material due to the presence of a tensile field at the crack tip. The present results can be explained if redistribution does not occur, the crack growing from a tensile field into a compressive field. Further investigations are underway to provide a more accurate residual stress distribution and resolve the apparent anomaly.

ACKNOWLEDGEMENTS

The authors would like to thank Prof. R.W.K. Honeycombe for the provision of laboratory facilities, Mr. A.J.A. Parlange and Dr. G.S. Booth of The Welding Institute for their advice and help with measuring residual stresses and Mr. C.A. Hipsley for his assistance with the PAZ simulation. Mr. J.E.M. Braid was supported by the Natural Sciences and Engineering Research Council Canada during the course of this work.

REFERENCES

- Adams, N.J.I. (1973). Crack growth in the vicinity of welds. *Welding Research International*, Nov., pp. 508s-513s.
- Clayton, J.Q. and Knott, J.F. (1974). University of Cambridge, Department of Metallurgy Report.
- Grey, T.G.F., Spence, J. and North, T.H. (1975). *Rational Welding Design*. Newnes-Butterworths, London.
- Macherauch, E. and Wohlfahrt, H. (1978). Different sources of residual stress as a result of welding. *Proc. Int. Conf. on Residual Stresses In Welded Construction and Their Effects*, Vol.1, The Welding Institute, Abington, Cambridge.
- Maddox, S.J. (1971). Fracture mechanics applied to fatigue of welded structures. *Proc. Conf. on Fatigue of Welded Structures*, Vol.1, The Welding Institute, Abington, Cambridge, pp.73-96.
- Ritchie, R.O., Garrett, G.G. and Knott, J.F. (1971). Crack-growth monitoring: optimisation of the electrical potential technique using an analogue method. *Int. J. Fract. Mech.*, 7, 462.
- Ritchie, R.O. and Knott, J.F. (1973). Mechanisms of fatigue crack growth in low alloy steel. *Acta Met.*, 21, pp.639-648.
- Rosenthal, D. and Norton, J.T. (1945). A method of measuring triaxial residual stress in plates. *The Welding Journal*.
- Segal, A. (1975). *Distribution and Deformation of Small Sulphide Inclusions in Steel*. Ph.D. Thesis, University of Cambridge.
- Underwood, J.H., Pook, L.P. and Sharples, J.K. (1977). Fatigue crack propagation through a measured residual stress field in alloy steel. *ASTM STP 631*, American Society for Testing and Materials.

TABLE 1. HY80 Plate Material

Composition %					
C	.18	Ni	2.89	S	.012
Mn	.35	Cr	1.67	P	.012
Si	.23	Mo	.51	Al	.013

Yield Stress	735 MPa at 23°C
UTS	895 MPa at 23°C
K_{IC}	182 $\text{MNm}^{-3/2}$ at 20°C (est. from δ_i (Clayton and Knott, 1974))